3D Imaging of a Phase Object from a Single Sample Orientation Using an Optical Laser

Chien-Chun Chen,[1] Huaidong Jiang,[2] Lu Rong,[1] Sara Salha,[1] Rui Xu,[1] Thomas G. Mason,[1,3] and Jianwei Miao[1*]

[1]*Department of Physics & Astronomy and California NanoSystems Institute, University of California, Los Angeles, CA 90095, USA.*

[2]*State Key Laboratory of Crystal Materials, Shandong University, Jinan 250100, People's Republic of China.*

[3]*Department of Chemistry and Biochemistry, University of California, Los Angeles, CA 90095, USA.*

We acquire coherent diffraction patterns of a microscale phase object at a single sample orientation by using an optical laser. The diffraction patterns are projected onto a spherical shell and then directly phased to obtain the 3D structure of the object. This imaging technique, known as ankylography, may potentially opens a door for 3D imaging of phase objects in the visible light region without the requirement of sample tilting or sectioning. In addition, using X-ray free electron lasers, this technique may be applied to determine the 3D structure of a certain class of objects without the need of identical copies. Finally, the extension of ankylography to more complicated and larger objects is suggested.

PACS numbers: 42.25.Fx, 42.30.Rx, 42.30.Wb, 87.64.M-

Lens-based microscopies, such as light, phase-contrast, fluorescence, confocal, x-ray and electron microscopy, have made important contributions to a broad range of fields in both physical and life sciences. In 1999, a new form of microscopy was developed,

termed coherent diffraction imaging, lensless imaging or coherent diffraction microscopy [1], in which the diffraction pattern of a non-crystalline specimen or a nano-crystal was first measured and then directly phased to obtain an image. The well-known phase problem was solved by oversampling the diffraction intensity [2] in combination of iterative algorithms [3-6]. Using synchrotron radiation, high harmonic generation, soft x-ray laser sources and free electron lasers, coherent diffraction imaging has been applied to conduct structure studies of a wide range of samples in materials science, nanoscience and biology [7-29]. To perform 3D coherent diffraction imaging, a sequence of 2D diffraction patterns has to be acquired by either tilting a sample at multiple orientations or using many identical copies of the sample [8,11,14,24,28]. In some application, however, it is very desirable to obtain the 3D structure of an object without the requirement of sample tilting or identical copies of the object. To achieve this challenging goal, a novel imaging method (ankylography) has recently been developed [30], which under certain circumstances allows for 3D imaging of an object from a single sample orientation. Subsequently, two imaging methods somewhat related to ankylography have been demonstrated. The first is super-resolution biomolecular crystallography [31], which under some conditions can determine the high-resolution 3D structure of macromolecules from low-resolution data. The other is discrete tomography [32], which enables to achieve the 3D atomic reconstruction of a small crystalline nanoparticle by only using two projections, combined with prior knowledge of the particle's lattice structure. Compared to conventional 3D structure and imaging methodology, these three methods are mathematically ill-posed problems, but represent a new and important direction in structural determination – retrieving 3D structural information from a portion of Fourier magnitudes or coefficients.

In this letter, we perform the ankylographic reconstruction of a phase object by using an optical laser. There are thee significant implications of this work. First, it extends ankylography to the 3D imaging of phase objects in the visible light region that is currently dominated by confocal microscopy. Second, compared to the previous result that is somewhat controversial due to the use of a transparent sample on an opaque substrate [33,34], this work represents the first ankylographic reconstruction of a phase object on a transparent substrate. Finally, using X-ray free electron lasers, ankylography may be applied to determine the 3D structure of a certain class of samples without the need of identical copies.

Figure 1 shows the schematic layout of the experimental setup. An optical laser with wavelength λ = 543 nm was collimated by a compound lens system, consisting of two converging lenses and producing a parallel beam with a diameter of ~200 μm. An aperture was placed 15 mm upstream of the sample to block the unwanted scatting from the lenses. The object to be imaged in 3D is a dielectric phase pattern made up of non-absorbing SU-8 epoxy photoresist that had been cross linked by using an Ultratech XLS stepper. Figure 2(a) shows a differential-interference-contrast (DIC) microscope image of the phase object, which consists of a dense arrangement of four alphabet letters (WWWA) in close proximity; as fabricated, the letters have about 1 μm thickness. The sample was supported on a Si_3N_4 membrane of 100 nm thick. To increase the depth of the sample along the Z (beam) axis, the Si_3N_4 membrane was tilted about 45° relative to the incident beam, creating a projection length of ~19 μm, ~23 μm and ~23 μm along the X-, Y- and Z-axes, respectively. Coherent diffraction patterns were recorded by a liquid-nitrogen-cooled CCD camera with 1340×1300 pixels and a pixel size of 20 μm × 20 μm, positioned at a distance

of 31.5 mm from the sample. A beamstop was positioned in front of the CCD detector to block the direct beam.

To obtain coherent diffraction patterns at highest possible resolution, we moved the CCD camera both horizontally and vertically, and measured a diffraction pattern at each of the four quadrants. The four diffraction patterns were tiled together to form a high resolution pattern. To ensure the missing center confined within the centro-speckle [35], we took a low-resolution diffraction pattern by moving the CCD camera further downstream at a distance of 108 mm to the sample. The high and low resolution diffraction patterns were combined to assemble a diffraction pattern with a small missing center. To remove the background scattering and readout noise of the CCD, we measured two sets of diffraction patterns at each position with the sample in and out of the laser beam. After subtracted the background, the diffraction patterns were assembled to form a 2D pattern with an array size of 2001 × 2001 pixels.

In order to perform ankylographic reconstructions, the diffraction patterns, measured by a planar CCD camera, have to be projected onto a spherical surface. As the solid angle subtended by each CCD pixel varies with the diffraction angle, the diffraction intensity was normalized by

$$I_N\left(k_x^d, k_y^d\right) = \frac{\Delta\Omega(0,0)}{\Delta\Omega\left(k_x^d, k_y^d\right)} I_M\left(k_x^d, k_y^d\right) \qquad (1)$$

where $I_N(k_x^d, k_y^d)$ and $I_M(k_x^d, k_y^d)$ are the normalized and measured diffraction intensities, (k_x^d, k_y^d) is the pixel position of the planar CCD, $\Delta\Omega(0,0)$ and $\Delta\Omega\left(k_x^d, k_y^d\right)$ are the solid angle subtended by the central pixel and pixel (k_x^d, k_y^d), respectively. $\Delta\Omega(k_x^d, k_y^d)$ is determined by,

$$\Delta\Omega\left(k_x^d, k_y^d\right) = R\int_{k_x^d-\delta/2}^{k_x^d+\delta/2}\int_{k_y^d-\delta/2}^{k_y^d+\delta/2}\frac{dk_x^d dk_y^d}{[(k_x^d)^2+(k_y^d)^2+R^2]^{3/2}} \qquad (2)$$

where R is the distance from the sample to the CCD camera and δ is the CCD pixel size.

The normalized diffraction intensity was then projected on the spherical surface on a Cartesian grid. To perform accurate interpolation, we first located the Cartesian grid points, (k_x^c, k_y^c, k_z^c), within a spherical shell of 1 voxel thick and then projected the grid points onto the planar CCD by

$$k_x^d{}' = R\frac{k_x^c}{R-k_z^c} \qquad k_y^d{}' = R\frac{k_y^c}{R-k_z^c}. \qquad (3)$$

where $(k_x^d{}', k_y^d{}')$ represent the X and Y coordinate on the detector plane that are not necessary an integer number of pixels. We calculated $I_N(k_x^d{}', k_y^d{}')$ by using the spline interpolation with the neighboring pixels, and then assigned $I_N(k_x^d{}', k_y^d{}')$ to the Cartesian grid point, $I_N(k_x^c, k_y^c, k_z^c)$. Figure 2(b) shows the diffraction intensity distributed within two spherical shells on a 3D Cartesian grid. The centro-symmetry of the diffraction intensity is because the sample is a phase object. The array size of the 3D Cartesian grid is 1691×1691×491 voxels with a diffraction angle of 32.3°.

To perform the ankylographic reconstruction, we first roughly estimated the support of the phase object. The algorithm was then iterated back and forth between real and reciprocal space. In real space, the electron density outside the support and the negative density inside the support were slowly pushed close to zero [5]. In reciprocal space, the Fourier magnitudes within the spherical shell were updated with the measure

ones while other Fourier magnitudes remained unchanged in each iteration. The convergence of the algorithm was monitored by an R_{sphere} defined as,

$$R_{sphere} = \frac{\left| |F^{M}_{sphere}(\vec{k})| - |F^{C}_{sphere}(\vec{k})| \right|}{|F^{M}_{sphere}(\vec{k})|} \qquad (4)$$

where $|F^{M}_{sphere}(\vec{k})|$ and $|F^{C}_{sphere}(\vec{k})|$ are the measured and calculated Fourier modulus within a spherical shell. Compared to the phase retrieval in coherent diffraction imaging, the convergence speed in the ankylographic reconstruction is slower and more iteration is required. After 5,000 iterations, we obtained a 3D reconstruction. By convolving the reconstruction with a Gaussian filter and choosing a cutoff value, we determined a tight support. The corresponding oversampling degree, defined as $O_d = N_{\text{shell}}/N_{\text{support}}$, is 2,062 [30], where N_{shell} and N_{support} are the voxel number within a spherical shell and the support, respectively. A large oversampling degree in the reconstruction is because the support used is very tight. After another 5,000 iteration, a final 3D reconstruction was obtained with R_{sphere} = 0.36. According to our experience, a correct, tight support is critical to the ankylographic reconstruction. In addition, a larger oversampling degree (O_d) is also helpful.

Figure 3(a) and a supporting movie [36] show iso-surface renderings of the ankylographic reconstruction. The orientation of the phase object relative to the beam is illustrated in Fig. 3(a). To verify the reconstruction, we tilted the reconstruction to the same orientation (Fig. 3b) as the DIC image (Fig. 2a). The 3 letters “WWW” are clearly visible and consistent with the DIC image, while the letter “A” is a bit too small to be resolved in the reconstruction. The resolution in ankylography is determined by $d_t = \lambda / \sin(2\theta)$ and $d_l = \lambda / (2\sin^2\theta)$, where d_t and d_l represent the transverse and

longitudinal resolution (*i.e*. perpendicular and parallel to the incident beam), and 2θ is the diffraction angle. In this experiment, the transverse and longitudinal resolution was estimated to be 1.0 μm and 3.5 μm, respectively. To further quantify the ankylographic reconstruction, we performed a line scan across the reconstruction (Fig. 3b). The blue curve in Fig. 3(c) shows the reconstructed density of the phase object, which is in reasonably good agreement with the DIC curve (the red curve). The discrepancy arises because ankylography produces the quantitative information of the phase object, but not the DIC image.

By using an optical laser, we measured coherent diffraction patterns from a phase object. The diffraction patterns were projected onto a spherical surface and then phased to obtain the 3D structure of the object. Transverse and longitudinal resolutions of 1.0 μm and 3.5 μm, respectively, were achieved. While the resolution is currently limited by the experimental set-up, the ultimate resolution is set by the wavelength of the incident beam. Compared to conventional coherent diffraction imaging [7-29], the ankylographic reconstruction not only requires a tight support with a large oversampling degree, but also becomes more challenging for larger objects. In order to apply ankylography to large objects, three different approaches are envisioned. First, our numerical simulations suggest that increasing the thickness of the spherical shell can distinctly improve the ankylographic reconstruction of large objects. Experimentally, this may be realized by using an incident wave with an energy bandwidth, coupled with an energy-resolved detector. Second, more real-space constraints can facilitate the ankylographic reconstruction of large objects. One way to achieve this is to position a 3D object with known structure close to an unknown one. Based on our numerical simulations, the combination of the known part and a

spherical diffraction pattern is more effective to reconstruct a large 3D object. Finally, by acquiring several spherical diffraction patterns at different sample orientations, ankylography can be extended to larger objects. Compared to conventional tomography, the number of projections required in ankylography will likely be much smaller due to the utilization of spherical diffraction patterns.

This work was in part supported by the U.S. Department of Energy, Office of Basic Energy Sciences (DE-FG02-06ER46276) and the U.S. National Institute of Health (GM081409-01A1). H. J. thanks the support by the NSFC of China (51002089), and Independent Innovation Foundation of Shandong University (2010JQ004).

*Corresponding author (Email: miao@physics.ucla.edu).

References

1. J. Miao, P. Charalambous, J. Kirz and D. Sayre, Nature **400**, 342 (1999).
2. J. Miao, D. Sayre and H.N. Chapman, J. Opt. Soc. Am. A. A **15,** 1662 (1998).
3. J. R. Fienup, Appl. Opt. **21**, 2758 ((1982)
4. V. Elser, Acta Cryst. A **59**, 201 (2003).
5. C. C. Chen et al., Phys. Rev. B **76**, 064113 (2007).
6. S. Marchesini, J. Opt. Soc. Am. A **24**, 3289 (2007).
7. I. K. Robinson et al., Phys. Rev. Lett. **87**, 195505 (2001).
8. J. Miao et al., Phys. Rev. Lett. **89**, 088303 (2002).
9. J. Miao et al., Proc. Natl. Acad. Sci. USA, **100**, 110 (2003).
10. D. Shapiro et al., Proc. Natl. Acad. Sci. USA **102**, 15343 (2005).
11. M. A. Pfeifer et al., Nature **442**, 63 (2006).
12. H. N. Chapman et al., Nature Phys. **2**, 839 (2006).

13. J. Miao et al., Phys. Rev. Lett. **97**, 215503 (2006).

14. G. J. Williams et al., Phys. Rev. Lett. **97**, 025506 (2006).

15. J. M. Rodenburg et al., Phys. Rev. Lett. **98**, 034801 (2007).

16. R. L. Sandberg et al., Phys. Rev. Lett. **99**, 098103 (2007).

17. B. Abbey et al., Nature Phys. **4**, 394-398 (2008).

18. H. Jiang et al, Phys. Rev. Lett. **100**, 038103 (2008).

19. P. Thibault et al., Science, **321**, 379 (2008).

20. C. Song et al., Phys. Rev. Lett. **101,** 158101 (2008).

21. R. L. Sandberg et al., Proc. Natl. Acad. Sci. USA, **105**, 24 (2008).

22. A. Barty et al., Nature Photon, **2**, 415 (2008).

23. Y. Nishino et al., Phys. Rev. Lett. **102**, 018101 (2009).

24. X. Huang et al., Phys. Rev. Lett. **103**, 198101 (2009).

25. E. Lima et al., Phys. Rev. Lett. **103**, 198102 (2009).

26. A. Ravasio et al., Phys. Rev. Lett. **103**, 028104 (2009).

27. A. P. Mancuso et al., Phys. Rev. Lett. **102**, 035502 (2009).

28. H. Jiang et al., Proc. Natl. Acad. Sci. USA, **107**, 11234 (2010).

29. Seibert et al., Nature **470**, 78 (2011).

30. K. S. Raines et al., Nature **463**, 214 (2010).

31. G. F. Schroder, M. Levitt and A. T. Brunger. Nature **464**, 1218 (2010).

32. S. Van Aert et al., Nature **470**, 374 (2011).

33. P. Thibault, Preprint at (http://arXiv.org/abs/0909.1643v1) (2009).

34. J. Miao, Preprint at (http://arXiv.org/abs/0909.3500v1) (2009).

35. J. Miao et al., *Phys. Rev. Lett*. **95**, 085503 (2005).

36. See EPAPS Document No._____ for supplementary information. This document can be reached through a direct link in the online article's HTML reference section or via the EPAPS homepage (http://www.aip.org/pubservs/epaps.html).

Figure Captions

Figure 1 Schematic layout of the experimental set-up. A compound lens system, consisting of two converging lenses, was used to collimate the incident laser beam with a wavelength of 543 nm. An aperture was placed 15 mm upstream of the sample to block the unwanted scatting from the lenses. A phase object made up of SU-8 epoxy photoresist was supported on a silicon nitride membrane of 100 nm thick. To increase the depth of the sample along the beam axis, the Si_3N_4 membrane was tilted about 45° relative to the incident beam. Coherent diffraction patterns were recorded by a liquid-nitrogen-cooled CCD camera with 1340×1300 pixels and a pixel size of 20 μm×20 μm, placed at a distance of 31.5 mm from the sample. A beamstop was positioned in front of the CCD camera to block the direct beam.

Figure 2 (**a**) DIC microscope image of the phase object, consisting of four alphabet letters (WWWA). (**b**) Two spherical diffraction patterns on a 3D Cartesian grid. The centro-symmetry of the two spherical patterns is because the sample is a phase object. The size of the 3D array is 1691×1691×491 voxels with a diffraction angle of 32.3°.

Figure 3 (**a**) Iso-surface rendering of the ankylographic reconstruction of the phase object where the relative orientation of the incident beam to the object position is illustrated. (**b**) The reconstruction is tilted to the same orientation as the DIC image (Fig. 2a). Although the resolution of the reconstruction is lower than the DIC image, the two images are in good agreement. (**c**) Line scans across the reconstruction and the DIC image. The two

curves agree reasonably well. The discrepancy arises because ankylography produces the quantitative information of the phase object, but not the DIC image.

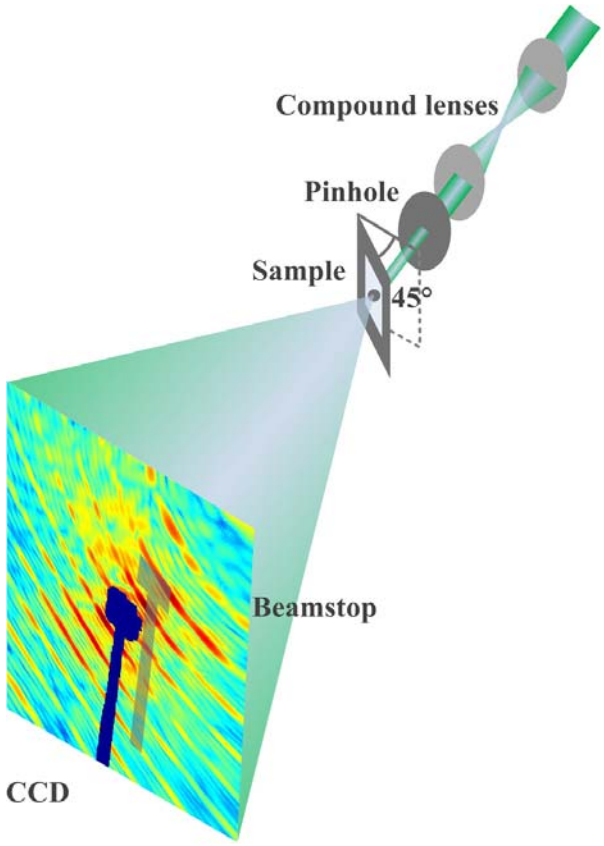

FIG. 1

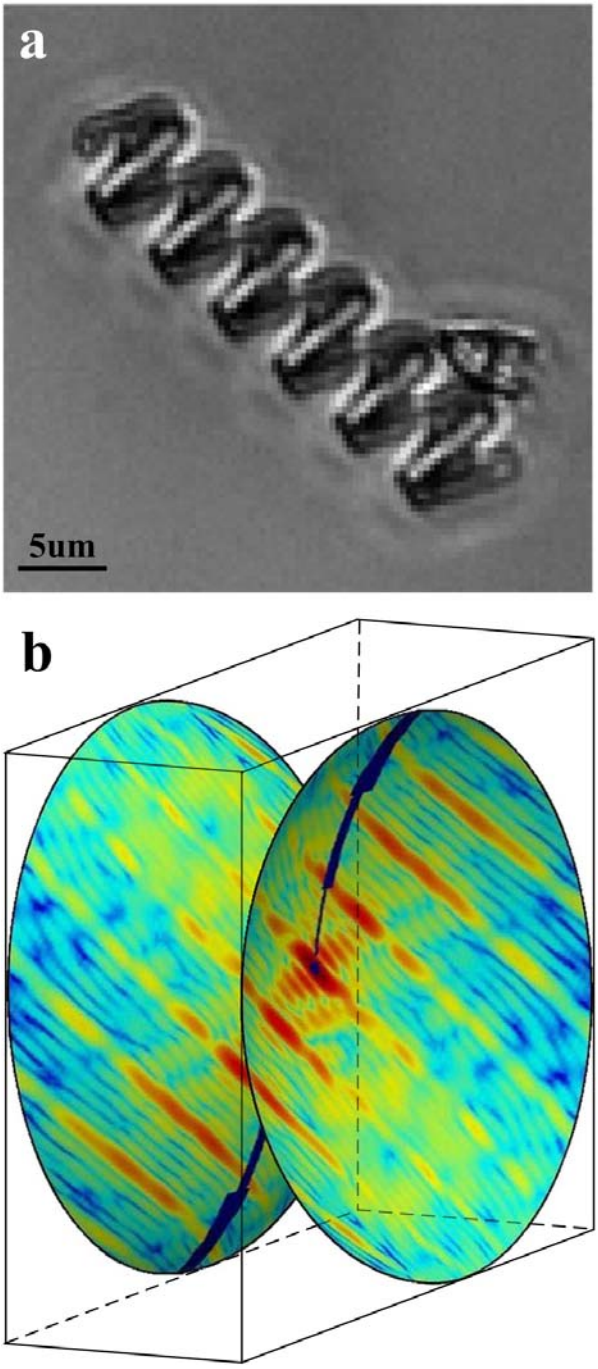

FIG. 2

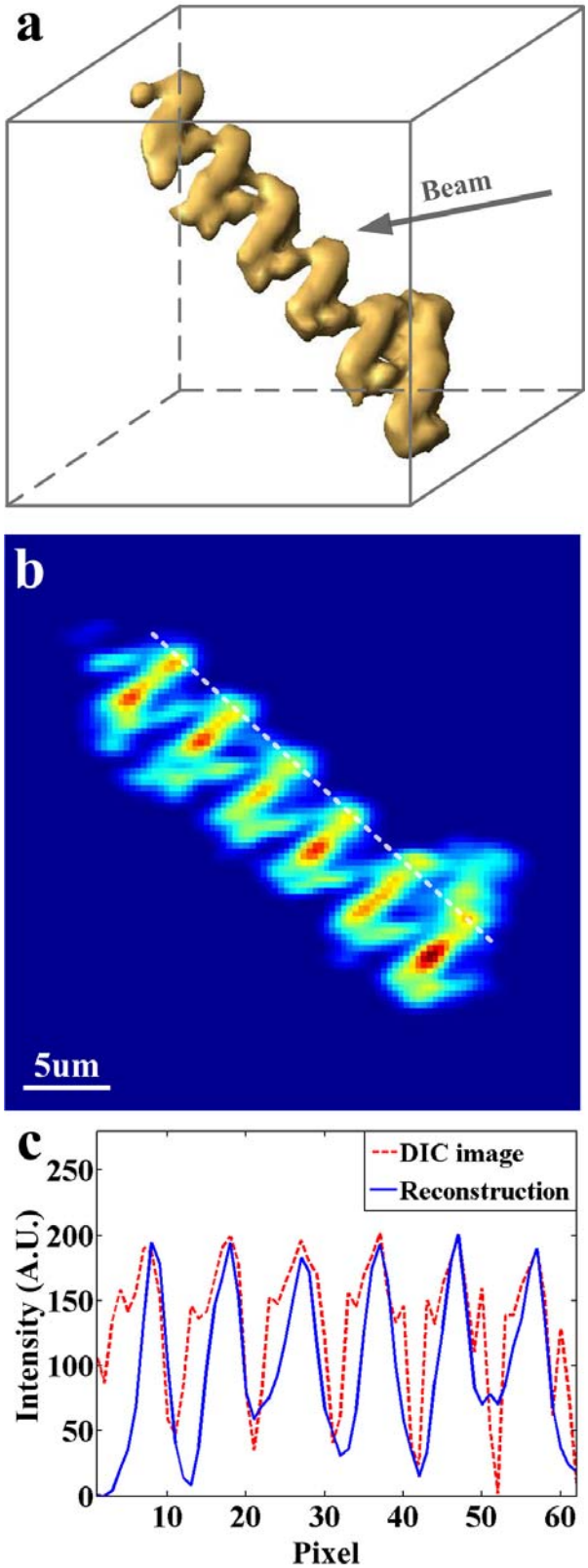
a
Beam
b
5um
c
DIC image
Reconstruction
Intensity (A.U.)
0
50
100
150
200
250
10
20
30
40
50
60
Pixel

FIG. 3